

INTRA UNDULATOR SCREEN DIAGNOSTICS FOR THE FERMI@Elettra FEL

M. Veronese*, A. Abrami, E. Allaria, M. Bossi, A. Buccioni, M. De Marco, L. Frölich, M. Ferianis, L. Giannessi, S. Grulja, R. Sauro, C. Spezzani, M. Tudor Sincrotrone Trieste, Trieste, Italy
T. Borden, Facility for Rare Isotope Beams, Michigan State University, East Lansing, MI, USA
F. Cianciosi, ESRF, Grenoble, France

Abstract

The FERMI@Elettra seeded FEL poses demanding requirements in terms of intra undulator diagnostics due to the short wavelength of its FEL radiation and to the co-existence of the electron and photon FEL beams. An advanced multi-beam screen system has equipped both FEL1 and FEL2. The system has been designed for transverse size and profile measurement on both the electron beam and the FEL radiation. Challenging design constraints are present: COTR suppression, seed laser suppression, FEL wavelength range and minimization of the ionizing radiation delivered to the undulators. This paper describes the novel design and the obtained performance with the FERMI intra undulator screen system (IU-FEL).

INTRODUCTION

FERMI@Elettra is a seeded FEL operating in the spectral range from VUV to soft x-rays [1]. It is based on a SLAC/BLN/UCLA type RF-gun, a normal conducting LINAC, currently operated at 1.2 GeV (up to 1.5 GeV). Longitudinal compression is provided by two magnetic chicanes BC1 and BC2 (respectively at 300 MeV and 600 MeV). The FEL has two undulator chains, namely FEL1 and FEL2. The first, FEL1, is a single cascade HGHG seed system designed to provide hundreds of microjoule per pulse in the range from 100 to 20 nm. The second, FEL2, is a double cascade seeded system designed to reach 4nm at the shortest wavelength. On both chains, in between the undulators several devices are installed: phase shifter, cavity BPM, a quadrupole and the intra undulator screen (IU-FEL). The IU-FEL screen is a multipurpose screen designed to provide transverse beam size measurements of the electron beam, the seed laser beam and the FEL beam. At present, seven stations are installed on the first FEL1 line and eight on the FEL2 line. The initial design of the system was performed in collaboration with Argonne National Laboratory. The setup presented in this paper has been deeply upgraded based on specific operational experience. Similar intra undulator diagnostics have been developed and tested at sFLASH at DESY [2].

GENERAL LAYOUT

The FEL1 and FEL2 chains are depicted in Figure 1. The FEL1 chain starts with the modulator where interac-

* marco.veronese@elettra.trieste.it

tion with the seed laser occurs. The modulator is followed by the dispersive section that converts the energy modulation in current modulation (bunching). The first IU-FEL station is installed downstream the dispersive section before the first radiator. This station is used, in conjunction with a standard multi-screen upstream the modulator, to perform a transverse alignment of the seed laser with the electron beam in order to guarantee the spatial overlap of the two beams in the modulator. This means that the IU-FEL screen should have the capability to image the electron beam and the seed laser at the same time. The other six IU-FEL stations are installed at each break in between the radiators. They provide imaging of both the electron beam and of the FEL electron beam with high resolution. The seed laser beam has a waist in the modulator, from there on the beam size increases due to its natural divergence. Moreover the vacuum chamber of the undulators has a vertical aperture of only 7 mm. This means that already after the second radiator the seed laser transverse profile is dominated by the reflection and diffraction from the vacuum chamber. In FEL2 the first cascade consisting of the modu-

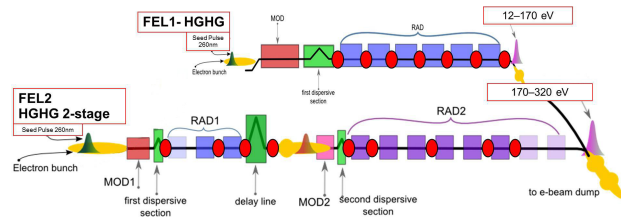


Figure 1: FERMI FEL1 and FEL2 layout. The IU-FEL stations are marked as red dots.

lator, the first dispersive section and the first two radiators, basically replicates the FEL1 chain. Downstream, the delay line is installed. It is a magnetic chicane that is used to delay the electron bunch with respect to the FEL radiation from the first stage. Zero delay would mean seeding with the FEL radiation emitted by the first stage on the same portion of the electron beam used for the first which has corrupted electron beam properties (emittance and energy spread). The delay line allows to seed on a fresh portion of the electron beam with unperturbed properties (fresh bunch technique). Downstream the delay line, a second modulator is installed and then a second dispersive section. From there the radiators of the second stage will amplify the bunching by the second dispersive section after the seeding process which now has also a shorter wavelength. The final

radiation wavelength of FEL2 is basically the wavelength of the seed laser (260 nm) divided by the harmonics number of the first stage and by the harmonic number of the second stage. In the final configuration, with an electron beam energy of 1.5 GeV this will allow the FEL2 chain to lase at wavelengths as short as 4 nm. IU-FEL stations are installed upstream and downstream the first modulator, downstream the delay line, the second dispersive section and at each second break between the second stage radiators, with a final station downstream of the last radiator.

DESIGN REQUIREMENTS AND CONSTRAINTS

The main electron beam parameters in all the stations are at present: energy of 1.25 GeV, charge of 500 pC, a projected emittance of about 2 mm mrad, a transverse electron beam size below 100 microns rms. The seed laser wavelength is 260nm with Ti:Sa (from 235nm to 265nm with the optical parametric amplifier). Seed energy per pulse is of several tens of microjoule. The FEL1 output energy downstream the last radiator has recently be measured as 300 microjoule at 52nm and has exceeded 20 microjoule at 20 nm. The energy per pulse emitted from the first radiator is a factor of 100 smaller than the one emitted at the last radiator.

For FEL1 several design constraints had to be considered designing the IU-FEL system. The requirements were multiple and often conflicting. The first requirement was to provide high resolution transverse imaging of the electron beam. The second task was to provide a transverse imaging of the FEL radiation. The third was to provide few stations with the capability of imaging at the same time the seed laser and the electron beam. The fourth goal was to provide pinholes in the IU-FEL screen which could be used to align by optical means all the emission from multiple undulators on the same line, to make easier the definition of the reference trajectory. The constraints in the design were multiple. First, a limited space was available since the whole intra-radiator section should be as short as possible, and a very limited space was available on the sides. This forced us to keep the vacuum chamber as short as possible and to develop the optics part below it. The second constrain, a machine protection issue [3], is to limit the radiation dose deposited in the undulators to few kGy over their lifetime to avoid demagnetization. This imposes the use of screen as thin as possible with small impact angles with the electron beam so that the effective thickness is kept as small as possible. Moreover materials with as low density and atomic number (Z) as possible were adopted. Finally coherent optical transition radiation (COTR) has been an issue too. Metallic screens could not be used for OTR diagnostics because the COTR would dominate and corrupt the information on the transverse distribution as seen also in LCLS [4] and SACLA [5]. Also using a scintillator like yttrium aluminum garnet doped with cerium (YAG:Ce), COTR is present although much weaker than for a metal-

lic scheme, so that suppression or mitigation strategies had to be adopted. Finally the same detection system had to measure both the electrons and the FEL radiation. YAG:Ce scintillators are used for both e-beam and FEL radiation but they have a different yield of visible photons, leading to an expected ratio of about 200. This constraint imposed to use full aperture of the iris of the lens objectives for the FEL, while using one inch neutral density filters with optical densities ranging from 1 up to 3.

VACUUM LAYOUT

The vacuum part consists of a small optical stainless steel tablet, on which all relevant component are mounted as shown in Figure 2. The assembly is moved transversely to the direction of propagation of the electron beam by an external stepper motor actuator. In Figure 2, three components are distinguishable. The first component top right is the setup used for e-beam diagnostics, the blue bottom component is a pinhole, the top left component is used for FEL diagnostics. Both the electron beam and the FEL beam generate fluorescence on a YAG:Ce. This visible radiation is imaged by an external detection system. The

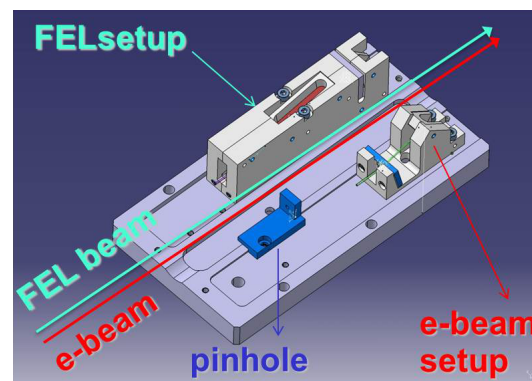


Figure 2: Vacuum optical tablet with the electron beam mount, the FEL mount and the pinhole.

electron beam setup is based on a new scheme that we developed. The standard YAG:Ce scintillators mounted at 45deg with respect to the electron beam and making a direct imaging of the scintillator surface have several limitations. The new scheme, shown in Figure 3 adopts a YAG:Ce 100 μm thick at quasi normal incidence. The scintillator surface is not imaged directly but by means of an in vacuum mirror which is displaced from the electron beam an set at an angle so that the optical axis is at normal incidence with respect to the surface of the YAG:Ce scintillator. This scheme has several advantages: the first is that the effective thickness is of only 105 μm reducing both the dose and the effect on the resolution due to the standard 45 degree layout. Moreover, there is no depth of field issue allowing for best performance of the optical also with fully open iris. Finally, since the nearest edge of the mirror is set at a distance above $10/\gamma$ no COTR radiation emitted by the YAG:Ce is collected. The FEL setup is depicted

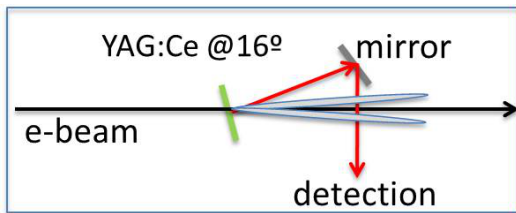


Figure 3: Electron beam setup scheme.

in Figure 4. The first mirror decouples the FEL radiation from the e-beam. The second mirror deflects the FEL radiation towards the YAG:Ce scintillator. The scintillator is imaged by means of an in vacuum mirror. Here the angles

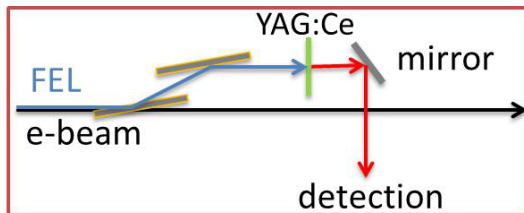


Figure 4: FEL beam setup scheme.

and the materials technology play a crucial role. The angle should be kept as large as possible to minimize the effective thickness of the material, but at the same time as small as possible allow for high reflectivity in the largest possible spectral range down to 10nm. The material used for the first mirror should have both low density and low Z to minimize its dose yield. To quantify the possible choices compatible with the available technological capabilities we have studied the dose deposited on the undulator by means of the code Fluka [6] for different materials (Cu, Be, Si SiO₂), thickness and angle. Figure 5 show an example calculation for Si of different thickness. The difference in the dose at the undulator is use huge (about a factor of 100) going from 0.1 mm thick copper at 2.5 degree of grazing angle, to 0.35 mm silicon at 10 degree. The reflectivity of the mirrors was also studied as a function of material (Cu, Be, Si, Au, and diamond) and angle (from 2.5 degree to 20 degree) using the CXRO code [7]. In Figure 6 we show the reflectivity of gold in the range from 10 to 40 nm for gold at 2.5 degree and at 10 degree. In both cases the reflectivity is pretty flat in the whole range and the relative difference is of 30%. In general, small angles would be preferable from the reflectivity point of view, while larger ones would be preferable from the machine protection point of view. The best compromise was found using silicon as a substrate, with a gold coating with a thickness 50 nm over a 5 nm bonding layer of chromium. The angle of incidence chosen is 10 deg to minimize the effective thickness but at the same time allow for good reflectivity down to a wavelength of 10 nm. There is an ongoing activity to test the performance of ultra-thin mirrors. Silicon 50 μ m mirrors have been installed with plans to test diamond ultra-thin mirrors. The second mirror

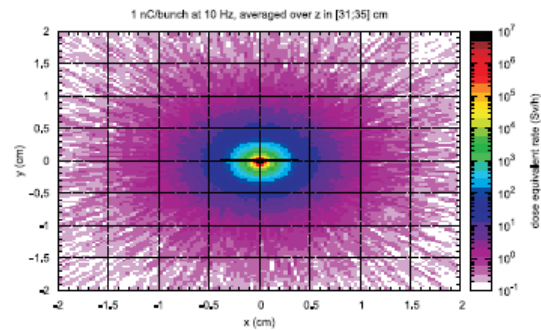
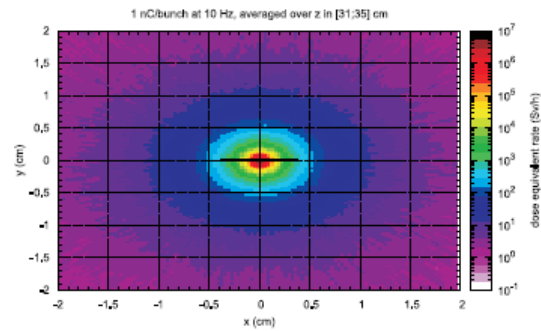


Figure 5: Simulation of dose generated by Si 300 μ m thick (upper plot) and by Si 50 μ m thick (lower plot).

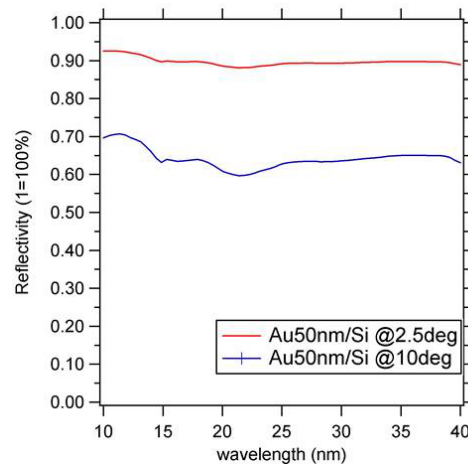


Figure 6: Simulation of dose generated by Si 300 μ m thick (upper plot) and by Si 50 μ m thick (lower plot).

is made of the same material and coating. The YAG:Ce has been coated with 90nm of aluminum to suppress the seed laser radiation co-propagating with the FEL and the COTR emitted by the first mirror.

OPTICAL LAYOUT

The detection part design is also based on some constraints: ideally a magnification (M) of about 1 is desired. The active area of the YAG:Ce is of 6mm. Together with $M \approx 1$ this defines the size of the CCD. The closest format commercially available is the 1/3 format. The design resolution of the system is 12 μ m rms, this requirement to

gether with the magnification leads to a pixel size of below $10\ \mu\text{m}$. The distance from the first lens to the targets is of about 210 mm. All this constrains have been met by using a Basler Scout 1300-32gm CCD combined with a Sigma MACRO 150 APO OS HSM lens used with fixed focus and full aperture iris installed with an extender tube of 1 inch to reach correct magnification. Since there is a focal distance difference of about 10 mm between the YAG:Ce of the electron beam setup and the YAG:Ce of the photon setup, the CCD and lens assembly has been installed on a motorized translation stage that is used to adjust the lens while keeping the magnification unchanged. As can be seen in Figure 7 the detection part is below the vacuum chamber and is composed of a rotating filter wheel, a 45 degree mirror, the lens attached to the CCD and mounted on the translation stage. The filters are of neutral density absorptive type, the diameter is of 1 inch. Each station is equipped with three filters with optical densities: 3, 2, and 1.3. Together with a clear aperture slot they provide the necessary dynamic range to the system to cope with the intensity difference of the image in the e-beam and FEL case.

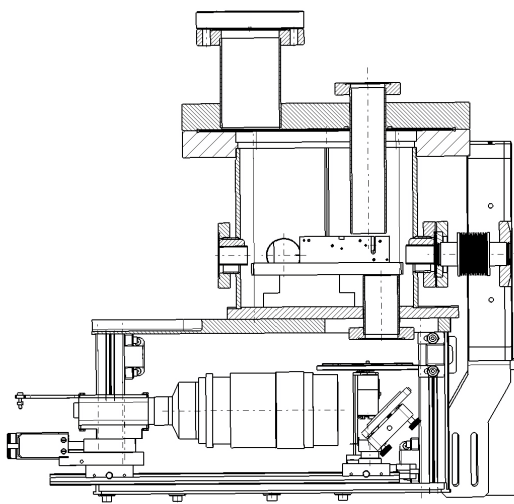


Figure 7: Layout of the optical in air detection part.

SEED VS EBEAM TRANSVERSE ALIGNMENT

The IU-FEL stations installed downstream the first dispersive magnets of FEL1 and FEL2 are used in conjunction with another multi-screen upstream of the modulator find the transverse overlap of the electron beam and the seed laser. This means that both beams should be imaged at the same time on a YAG:Ce. The typical situation before and after alignment is shown in Figure 8. The image on the left shows the two beams on the YAG:Ce not overlapped. The e-beam is the bright upper right spot while the seed laser is the dimmer lower left spot. The image on the right shows

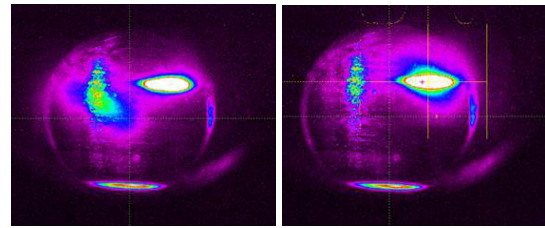


Figure 8: Transverse alignment of the seed laser to the electron beam. The left image shows unaligned beams. The seed laser spot being the dimmer spot on the left while the e-beam is the brighter spot on the upper right. The right image shows seed laser and the e-beam transversely overlapped.

the two beams overlapped. The seed laser intensity is attenuated to the level of 1 microjoule to avoid possible damage to the YAG:Ce crystal.

ELECTRON BEAM MEASUREMENTS

The main goal of the electron beam side of the system is to check whether the electron beam optics provides the desired FODO to keep the transverse dimension of the electron beam small all along the undulator chain to guarantee optimal overlap of the FEL radiation with the electron beam. For this reason a good resolution is needed. Figure 9 shows the image of the smallest horizontal size of the FERMI electron beam in the last IU-FEL station of FEL1 acquired during a resolution test of the diagnostics with specific manual tuning of the quadrupole. The Gaussian fitting of the measure spot size profile has a sigma of $15\ \mu\text{m}$. It should be noted this is well below the standard operational setting of the FEL. This result is in line with the modulation transfer function test on the detection system measured in the optical laboratory to be about 120 lp/mm. The COTR mitigation strategy worked as expected since

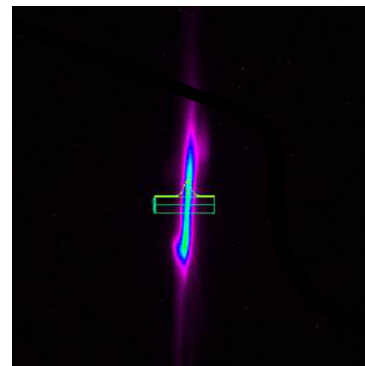


Figure 9: Image of electron beam on YAG:Ce with beam optics optimized to minimum horizontal electron spot size. The horizontal profile has a Gaussian rms width of $15\ \mu\text{m}$.

none of the usual COTR effects (image pattern distortion like donut shape or other and intensity fluctuations) were recorded.

FEL BEAM MEASUREMENTS

FEL radiation transverse pattern measurement can be made shot by shot downstream of the last three radiators, while for the first three a multi shot average is needed since the FEL power is pretty low in the first part of the FEL chain. As an example of the system capabilities we report in the figures 10 and 11 the FEL radiation patterns measured downstream of the last undulator with FEL1 tuned at 43 nm. The first image shows the pattern with the last undu-

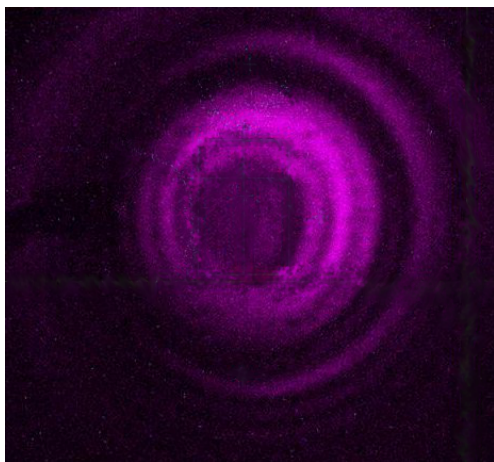


Figure 10: FEL radiation at 43nm as measured downstream the last undulator of FEL1 with the last radiator open.

lator open, the second one with the last undulator closed. Not only the central cone of radiation is more intense in the latter case as expected, but also the fringe structure is changed. We attribute the fringes to interference from the different undulators.

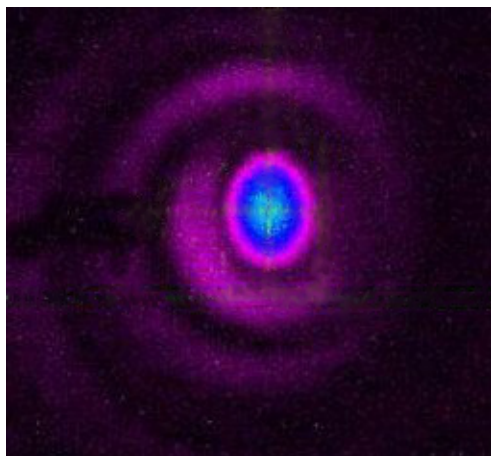


Figure 11: FEL radiation at 43nm as measured downstream the last undulator of FEL1 with the last radiator set on resonance.

PINHOLES

The optimal alignment between FEL and electron beam is not a trivial task, and beam based alignment (BBA) is needed but not always sufficient. To define a straight trajectory, as done in other labs (see [5]), we decided to install also pinholes in the IU-FEL vacuum system as shown in Figure 2. Since the seed laser divergence and diffraction makes it very quickly unusable as an alignment laser as the distance from the waist increases, we will use pinholes. The idea is to use each pinhole in the Nth station as a diffraction source and image the pattern on the downstream YAG:Ce screen in station (N+1). To ease the work we decided to use only the central lobe of the Airy diffraction pattern of a pinhole. Given the pinhole-screen distance, the 260 nm seed laser wavelength the resulting pinhole diameter is 1.5 mm. The operational experience so far with the pinhole has shown their capability of highlighting inconsistencies in the alignment performed with the laser tracker.

ACKNOWLEDGMENT

We would like to thank J.Noohnan and D.Walters of Argonne National Laboratory, as well as G. Ciani for the initial design of the system. M. Lazzarino of CNR-IOM laboratory for the thin film coating of both mirrors and YAG:Ce. R.Tamara for very accurate preparation of high precision components. This work was supported in part by the Italian Ministry of University and Research under grants FIRB-RBAP045JF2 and FIRB-RBAP-6AWK3.

REFERENCES

- [1] E. Allaria et al., "Highly coherent and stable pulses from the FERMI seeded free-electron laser in the extreme ultraviolet", *Nature Photonics* advance online publication, 23 September 2012 (doi:10.1038/nphoton.2012.233).
- [2] J. Bödewad et al., MOPD54, Proceedings of DIPAC2011, Hamburg, Germany (2011).
- [3] L. Fröhlich et al., The machine protection system for FERMI@Elettra. Proc. FEL'10, pp. 667670, Malm, Sweden, August 2010.
- [4] J. Frisch et al. THBAU01, Proceedings of FEL2008, Gyeongju, Korea (2008).
- [5] T. Hara et al., TUPA26, Proceedings of FEL2011, Shanghai, China (2011).
- [6] "FLUKA: a multi-particle transport code", A. Ferrari, P.R. Sala, A. Fassio, and J. Ranft, CERN-2005-10 (2005), INFN/TC_05/11, SLAC-R-773.
- [7] CXRO, http://henke.lbl.gov/optical_constants/